(NASA-CR-199626) DETERMINATION OF   N96-14296
THE DISPERSION CONSTANT IN A
CONSTRAINED VAPOR BUBBLE
THERMOSYPHON (Indian Inst. of   Unclas
Tech.) 8 p

                                      G3/34 0076338

$N A G 3 - 1399$

$I N - 34 - C R$

5491

$p.8$

DETERMINATION OF THE DISPERSION CONSTANT IN A CONSTRAINED VAPOR BUBBLE THERMOSYPHON

Sunando DasGupta
Indian Institute of Technology, Kharagpur
Kharagpur-721 302
India

Joel L. Plawsky and Peter C. Wayner, Jr.
The Isermann Department of Chemical Engineering
Rensselaer Polytechnic Institute,
Troy, New York 12180-3590

ABSTRACT

The isothermal profiles of the extended meniscus in a quartz cuvette were measured in a gravitational field using an image analyzing interferometer which is based on computer enhanced video microscopy of the naturally occurring interference fringes. The experimental results for heptane and pentane menisci were analyzed using the extended Young-Laplace Equation. These isothermal results characterized the interfacial force field in-situ at the start of the heat transfer experiments by quantifying the dispersion constant, which is a function of the liquid-solid system and cleaning procedures. The experimentally obtained values of the disjoining pressure and the dispersion constants were compared to that predicted from the DLP theory and good agreements were obtained. The measurements are critical to the subsequent non-isothermal experiments because one of the major variables in the heat sink capability of the Constrained Vapor Bubble Thermosyphon, CVBT, is the dispersion constant. In all previous studies of micro heat pipes the value of the dispersion constant has been "estimated". One of the major advantages of the current glass cell is the ability to view the extended meniscus at all times. Experimentally, we find that the extended Young-Laplace Equation is an excellent model for the force field at the solid-liquid-vapor interfaces.

NOMENCLATURE

$\bar{A}$	=	modified Hamaker constant (J).
B	=	dispersion constant (J m).
C_1	=	constant of integration, Eq. (9).
Δy	=	hydrostatic head difference.
K	=	curvature (m^{-1}).
n	=	refractive index.

Q	=	heat input, (W)
x	=	distance, (m).
Z	=	dimensionless distance, Eq. (5)
α	=	dimensionless variable, Eq. (7).
δ	=	film thickness, (m).
δ_0	=	adsorbed film thickness.
η	=	dimensionless film thickness, δ/δ_0.
Π	=	disjoining pressure/length, (N/m^3).
σ	=	surface tension, (N/m).

Subscript

l	=	liquid.
s	=	solid.
v	=	vapor.
Y-L	=	Young-Laplace equation.
∞	=	denotes thicker portion of the meniscus.

INTRODUCTION

When the gravitational body force is essentially removed, the shape of a constrained liquid volume with a free interface in a container changes dramatically to reflect the new force field. The resulting equilibrium shape under microgravity conditions depends on the intermolecular force field which changes rapidly in the vicinity of the liquid-vapor and liquid-solid interfaces. Under non-equilibrium conditions, microgravity fluid dynamics and change of phase heat transfer are functions of further changes in the shape of the fluid volume from its equilibrium shape. Therefore, in small systems, the shape dependent interfacial intermolecular force field can be used to control fluid flow and heat transfer (Derjaguin et al., 1965, Potash and Wayner, 1972, Wayner et

$$P_v = P_l + \sigma K + \frac{(-B)}{\delta^n}$$

VAPOR

VAPOR FLOW

LIQUID FLOW

SOLID BARRIER

LIQUID FILM, THICKNESS = $\delta(x,\theta)$

VAPOR

① v_1 (a)   (b)   (c) v_2 ②

CONDENSATION   EVAPORATION

$$T_2 > T_1$$
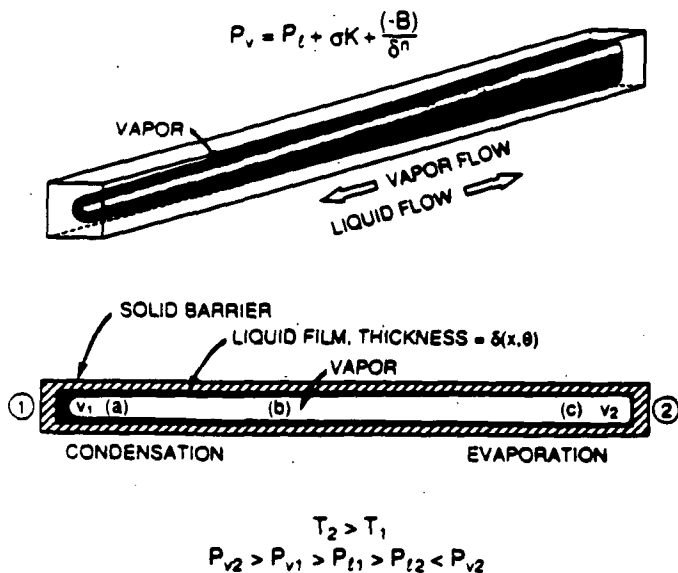$$P_{v2} > P_{v1} > P_{l1} > P_{l2} < P_{v2}$$

FIGURE 1 CVBT CONCEPT.

al., 1976). The initial equilibrium liquid film shape is controlled by fixing the container shape, the liquid and solid substrate surface properties, and the volume of the liquid.

In particular, we are concerned with the experimental study of the generic constrained vapor bubble thermosyphon (CVBT) system presented in Fig. 1. For a completely wetting system, the liquid will coat all the walls of the chamber. For a finite contact angle system, some of the walls will have only a small amount of adsorbed vapor which changes the surface properties of the solid-vapor surface. Liquid will fill a portion of the corners in both cases. If temperature at End (2) is higher than End (1), because of an external heat source and sink, energy flows from End (2) to End (1) by conduction in the walls and by an evaporation, vapor flow and condensation mechanism. The condensate flows from End (1) to End (2) because of the intermolecular force field which is a function of the film profile. A CVBT with a very small cross section has been called a micro heat pipe (Cotter, 1984).

There is a "pressure jump" at the liquid-vapor interface, due to the anisotropic stress tensor near interfaces. For many years, the classical Young-Laplace equation of capillarity has been successfully used to describe the pressure jump at a curved liquid-vapor interface. An example of its use to describe the fluid dynamics in a micro heat pipe is given in a publication by Wu and Peterson (1991). In this case, the pressure jump is a function of the liquid-vapor surface tension and the interfacial radius of curvature. However, near the liquid-solid interface, additional changes in the stress field within the liquid occur because of changes in the intermolecular force field due to solid molecules replacing liquid molecules. This leads to the augmented Young-Laplace model for the pressure jump at the liquid-vapor interface (Derjaguin and Kussakov, 1939, Potash and Wayner, 1972, Derjaguin and Churaev, 1976, Teletzke et al., 1976, Renk et al., 1978, Kamotani 1978, Holm and Goplen, 1979, Moosman and Homsy, 1980, Truong and Wayner, 1987, DasGupta et al., 1993a). These long range van der Waals forces have been found to be extremely important in that they lead to the concept of an extended evaporating meniscus

(Potash and Wayner, 1972, Wayner et al., 1976). In a completely wetting system, a thin adsorbed film extends for a long distance beyond the classical equilibrium meniscus (Derjaguin et al., 1965, Wayner, 1991). The thin film controls the important processes of spreading and wetting. It forms a thin liquid bridge between the "classical menisci" formed in the corners of the chamber presented in Fig. 1. Recently Khrustalev and Faghri (1993) and Swanson and Peterson (1993) have used this type of model to analyze a micro heat pipe. Heat transfer from a stable evaporating thin film in the neighbourhood of a contact line was analyzed by Brown et al., (1993). Swanson and Herdt (1992) have used the three dimensional augmented Young-laplace equation to develop a mathematical model describing the evaporating meniscus in a capillary tube. Herein, we present the initial experimental results of a study of the three dimensional extended meniscus in a configuration of general importance to the microgravity environment : the constrained vapor bubble thermosyphon.

The effects of both the liquid-vapor and liquid-solid interfaces on the effective pressure jump at the liquid-vapor interface of the extended two dimensional meniscus have been modeled using the following augmented Young-Laplace equation :

$$P_l - P_v = \frac{B}{\delta^n} - \sigma K$$

$$\frac{B}{\delta^n} = \frac{B}{\delta^4} = -\Pi, \qquad \delta \geq 40 \text{ nm} \qquad (1)$$

$$\frac{B}{\delta^n} = \frac{\overline{A}}{\delta^3} = -\Pi \qquad \delta \leq 20 \text{ nm}$$

where P_l is the liquid pressure, P_v is the vapor pressure, $\overline{A}$ is the Hamaker constant (negative for a completely wetting liquid), B is the retarded dispersion constant for thicker films, $\delta(x)$ is the film thickness, K is the curvature and σ is the surface tension. The first term on the right hand side of Eq. (1) is called the disjoining pressure, $-\Pi$, and it represents the change in the body force on the liquid due to the long range van der Waals forces between the liquid and solid over a narrow range of thicknesses.

According to Eq. (1), the effective pressure in the liquid is reduced below that in the vapor by both capillarity and disjoining pressure in a completely wetting system. This leads to a reduction in the vapor pressure. However, the vapor pressure reduction can be offset by a temperature increase to obtain the vapor bubble thermosyphon presented in Fig. 1. The chemical potential field is a function of the temperature and the effective liquid pressure which is a function of the shape of the liquid film. Therefore, the process is understood by measuring the temperature field and the liquid film shape.

Theory

The augmented Young-Laplace equation can be written for a point in the thicker portion of the meniscus, where the disjoining pressure effects are negligible and for another
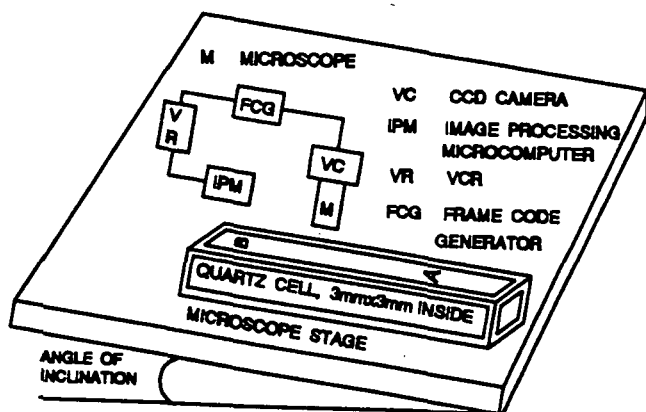
FIGURE 2 SCHEMATIC DIAGRAM OF THE EXPERIMENTAL SET-UP.

FIGURE 3 INTERFERENCE FRINGES AND THE GREY VALUE PLOT.

is shown in Fig. 2. The cell was essentially a small cuvette, made of quartz to facilitate optical observation and measurement of the liquid meniscus. The prototype cell was square (3mm x 3mm inside) in cross section, as is the case with the actual CVBT. The actual CVBT being made is slightly more complicated to facilitate the cleaning (it has a vacuum port, a pure test liquid feed port) and it is made of a special high refractive index glass to enhance the contrast for optical measurements. The present study was conducted as a precursor to the non-isothermal CVBT experiments, mainly to develop the method for accurately measuring the liquid film thickness profile and to estimate the dispersion constant, in situ, at the start of the experiment. The isothermal results characterize the interfacial force field and the information are critical to the operation and the heat sink capability of the CVBT.

The film thickness profile at the corners of the experimental cell was measured using IAI - image analyzing interferometry. Interference phenomena were used to determine the profile of the capillary meniscus in the thickness range $\delta \geq 0.1 \mu m$. A detailed description of the IAI techniques and hardware for film thickness profile measurement were presented in DasGupta et al. (1993, 1994) and DasGupta et al. (1991).

The cell was partially filled up with the liquid and placed on the microscope stage. The whole assembly was tilted with respect to the horizontal at two different angles in the two settings used in this study. The system was left to equilibrate with the surroundings for 3 hours before taking any data. An optical interference pattern representing the thickness profile was readily observed (Fig. 3). The pictures of the interference patterns formed at the corners of the cell at two specific points (A and B, as shown in Fig. 2) for each angle setting were captured in the image processor. From each image a plot of the pixel grey value versus distance was extracted. The grey value at each pixel was a measure of the reflectivity. As is evident from Fig. 3, the reflectivity underwent a cyclic change with increase in film thickness. The computer
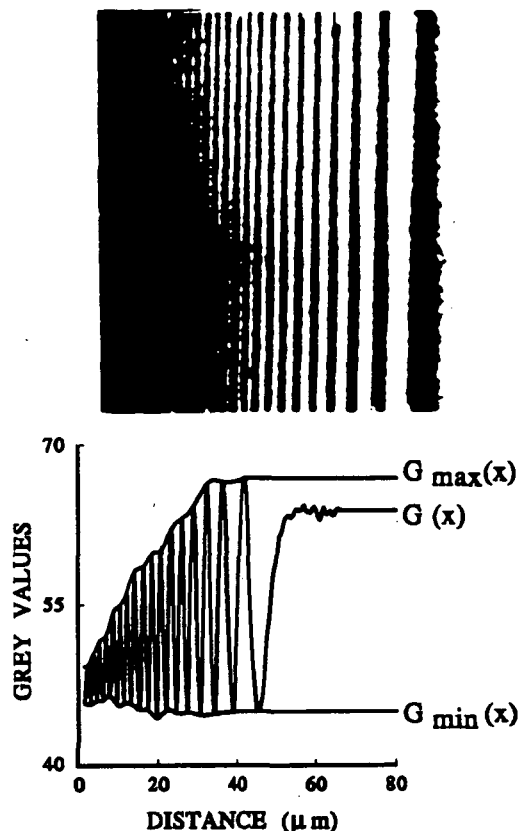
program scanned the peaks and valleys and filtered the noise from the real peaks/valleys. It then interpolated peak/valley envelopes and by analyzing the relative reflectivity of any pixel with respect to these (dark and light pixel envelopes), determined a film thickness at every pixel (DasGupta et al., 1991). The fact that the extended capillary meniscus merged smoothly to an adsorbed flat film was utilized to estimate the adsorbed film thickness from the grey value data and the peak/valley envelopes. The adsorbed film is obvious in the grey value plot since $G(x) < G_{max}(x)$ in the region $x > 50 \mu m$. In our previoius studies, the estimated error in measuring the adsorbed film thickness was $\pm 0.5 nm$-$1.0 nm$ for the thickness range studied on a reflecting Silicon substrate (DasGupta, et al., 1993, 1994). This high degree of accuracy was possible because a complementary ellipsometer was used to measure δ_0. Viewing the film through the quartz wall does not allow the same level of accuracy because the complementary ellipsometer is not used. Therefore, the value of δ_0 is estimated using the size of gap between G_{max} and $G(x)$ in the flat thin film region presented in Figure 3. An estimation of the overall error associated with the results can be obtained by viewing the final results presented below in Figure 8. This error also includes local variations in the intermolecular forces at the liquid-solid interface.

Figure 4 and 5 are two examples of the measured film thickness profiles with heptane as the test liquid. Each picture

point where both effects are present. For the isothermal non-evaporating (Q=0) cases considered here, the liquid pressure will remain the same, irrespective of the position. In the earths gravitational field, the following equation applies at a fixed hydrostatic head.

$$\sigma K - \frac{B}{\delta^4} = \sigma K_\infty \quad , Q = 0 \tag{2}$$

We note that the curvature at the thicker portion of the meniscus (K_∞) is nearly constant (DasGupta et al., 1993b). In Eq. (2), the curvature (K) can be expressed in the following form.

$$K = \frac{\frac{d^2\delta}{dx^2}}{[1 + (\frac{d\delta}{dx})^2]^{3/2}} \tag{3}$$

Using a simplified form of curvature, which is valid only if the square of the slope is small compared to one, Eq. (2) can be written in the following way.

$$\sigma \frac{d^2\delta}{dx^2} - \frac{B}{\delta^4} = \sigma K_\infty \tag{4}$$

For the isothermal experiments reported in this study the value of the maximum slope is 0.15 and hence using the simplified form of curvature is justified. The following variables are introduced next to modify Eq. (4) to obtain Eq. (6).

$$\eta = \frac{\delta}{\delta_0} \qquad Z = x \left(\frac{K_\infty}{\delta_0}\right)^{1/2} \tag{5}$$

$$\frac{d^2\eta}{dZ^2} + \left(\frac{-B}{\sigma K_\infty \delta_0^4}\right) \frac{1}{\eta^4} = 1 \tag{6}$$

Eqs. (2 - 6) are valid for an _equilibrium situation_ where no evaporation or condensation is taking place. A dimensionless variable, α, is defined next.

$$\alpha^4 = \frac{-B}{\sigma K_\infty \delta_0^4} \tag{7}$$

Eq. (6) can now be written as

$$\frac{d^2\eta}{dZ^2} = 1 - \frac{\alpha^4}{\eta^4} \tag{8}$$

For the equilibrium case, Q=0 and α=1. Any values of α other than unity will signify deviation from the equilibrium situation. The experimental section of the paper and the

subsequent discussion will present two experimental cases, which were very close to equilibrium. The results will demonstrate the utility of the model and the evaluation of the values of α.

After multiplying both sides of Eq. (8) by 2dη/dZ and integrating (C_1 is the constant of integration),

$$\left(\frac{d\eta}{dZ}\right)^2 = 2\eta + \frac{2}{3} \frac{\alpha^4}{\eta^3} + C_1 \tag{9}$$

The boundary condition used for the completely wetting case is

$$\text{For} \qquad \eta = \alpha \qquad \frac{d^2\eta}{dZ^2} = 0 = \frac{d\eta}{dZ} \tag{10}$$

Note that this can be viewed as an artificial boundary condition for a non-equilibrium system for which $\alpha > 1$. The utility of the extended model is demonstrated below.

Using the boundary condition, the slope of the meniscus can be expressed as

$$\frac{d\delta}{dx} = -(K_\infty \delta_0)^{1/2} \sqrt{2\eta + \frac{2}{3} \frac{\alpha^4}{\eta^3} - \frac{8}{3} \alpha} \tag{11}$$

Hence if the curvature at the thicker end of the meniscus, K_∞, along with B, δ_0 and σ are known, the slope of the meniscus can be directly calculated as a function of the film thickness, using only the augmented Young-Laplace equation. The minus sign in Eq. (11) is indicative of the fact that for the reference frame selected, the meniscus slope should always be negative (film thickness decreases as distance increases). In a recent publication DasGupta et al. (1994) have demonstrated that the augmented Young-Laplace equation can be successfully used to evaluate the slope profiles for isothermal cases from known values of K_∞, B, δ_0 and σ. Their results clearly demonstrated the validity of the augmented Young-Laplace equation to predict the equilibrium meniscus shape.

Herein we compare the slope of the meniscus obtained by numerical analysis of the experimental data for a system with unknown values of Hamaker constant (or dispersion constant, depending on the adsorbed film thickness) and the slope predicted by the augmented Young-Laplace equation (Eq. 11). The slope predicted by Eq. (11) is a function of α and the α corresponding to the closest match between these two slopes is selected to determine the value of the dispersion constant for the CVBT, in situ, for our isothermal experiments, as will be apparent in the next sections. Finally we compare the experimentally obtained values of the dispersion constants and the disjoining pressures with the predictions from the DLP theory (Dzyaloshinskii et al., 1961) for our experimental system.

EXPERIMENTAL

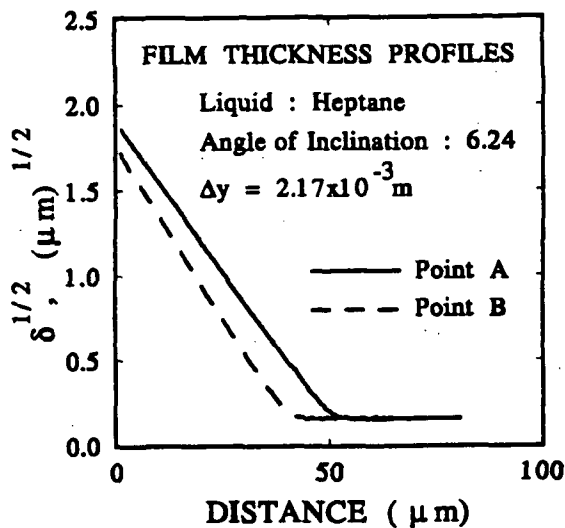A schematic diagram of the cell and the experimental set up

FIGURE 4 FILM THICKNESS PROFILES OF HEPTANE AT DIFFERENT POSITIONS (POINT A AND B) FOR AN ANGLE OF INCLINATION EQUAL TO 6.24°.

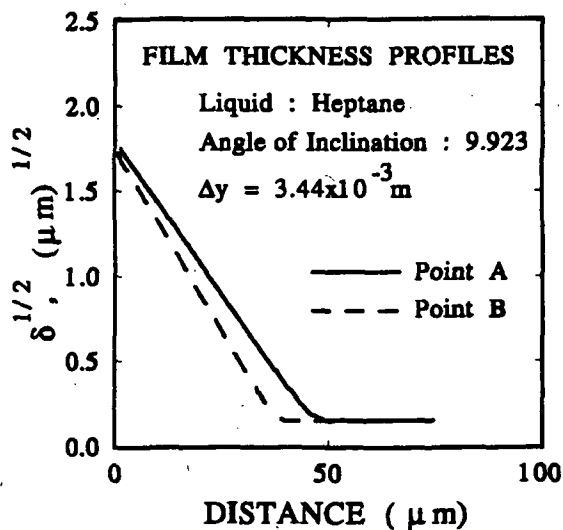FIGURE 6 COMPARISON BETWEEN THE EXPERIMENTAL SLOPE AND EQUATION (11).

FIGURE 5 FILM THICKNESS PROFILES OF HEPTANE AT DIFFERENT POSITIONS (POINT A AND B) FOR AN ANGLE OF INCLINATION EQUAL TO 9.92°.
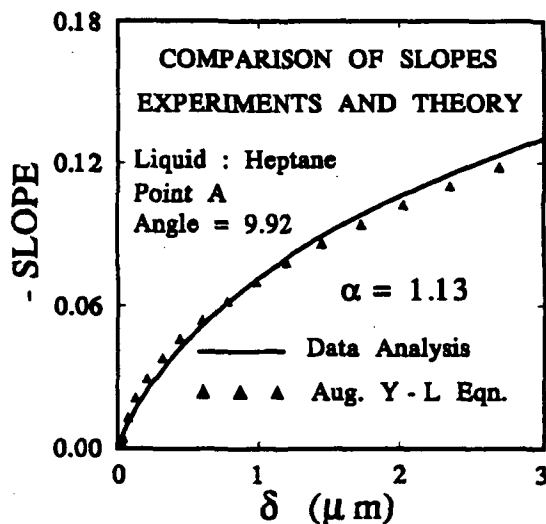
FIGURE 7 COMPARISON BETWEEN THE EXPERIMENTAL SLOPE AND EQUATION (11).

was for a specific angle. In an isothermal system of spreading liquid on an inclined solid substrate the curvature should remain constant in the region where dispersion forces can be neglected. So the film profile in this range approximated a parabola and a plot of $\delta^{1/2}$ vs x was a straight line. As can be seen form Figs. 4 and 5, $\delta^{1/2}$ vs x was nearly a straight line in all the cases, showing the proximity of the cases to isothermality. On the other hand it is clear form these figures that the thickness profiles at point B in each of these angle
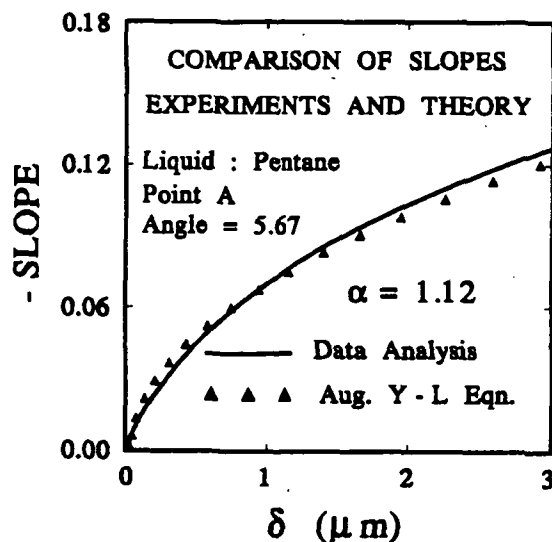
settings were steeper than in point A as a result of higher hydrostatic pressures and subsequent higher curvatures. Again a comparison of Fig. 4 and 5 demonstrates that, as expected, an increase in angle resulted in an increase in the film curvature. Plotting $\delta^{1/2}$ vs x, therefore, clearly illustrates the sensitivity of the film thickness shape to externally imposed conditions. This will not be obvious from a plot of δ versus x. In addition, the adsorbed film thickness, δ_0, is clearly seen in the region x≥50μm. Next we address the significance of the film thickness profile measurements.

RESULTS AND DISCUSSION

The objective of this work is to characterize the interfacial force field by evaluating the dispersion constant, in situ, for the solid-liquid-vapor system. Once the film thickness profile and the adsorbed film thickness were obtained, the curvature at the thicker end of the meniscus was determined. Equation (11) was then used to calculate the slope of the thickness profiles as a function of α and the α corresponding to the closest match between the experimental slope, obtained by numerical differentiation of a cubic spline fitted to the data, and Eq. (11) was used to determine the dispersion constant for the specific liquid-solid system.

Figures 6 and 7 show two pictures of the close match between the experimental slope and the slope obtained by the solution of the augmented Young-Laplace equation. The triangles represent the slope at every tenth point obtained by data analysis, whereas the solid line represents the solution of the augmented Young-Laplace equation for the specific value of α. Table 1 summarizes the results for the two liquids in the small cell.

The values of the dispersion constants for the quartz-pentane-vapor system are presented in Table 1. Similar results were also obtained for heptane. The dispersion constants are calculated from the known values of α corresponding to the minimum error. The values of B for each liquid are reasonably close to each other. We also calculated the dispersion force and the values of B from the DLP theory for quartz-pentane-vapor and quartz-heptane-vapor systems. To calculate the dispersion force from the DLP theory, the same methodology developed by Truong and Wayner (1987) and Gee et al. (1989) is used. The dielectric functions of the liquids and quartz are obtained from spectroscopic optical data as described by Hough and White (1980). The results are presented in Table 2 and in Fig. 8. Figure 8 is a plot of the disjoining pressure as a function of the film thickness for heptane wetting on quartz. The solid line is from DLP theory,
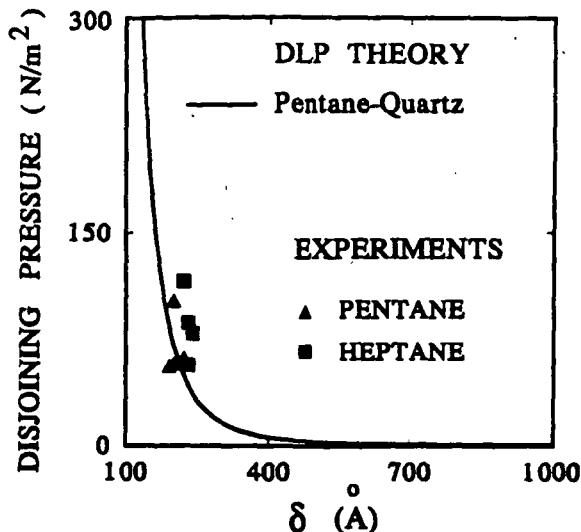

FIGURE 8 COMPARISON BETWEEN THE DLP THEORY AND EXPERIMENTS FOR THE ADSORPTION OF PENTANE AND HEPTANE ON QUARTZ.

whereas the symbols are from the experiments. Since the values of the dispersion forces for the two alkanes on quartz, as predicted by the DLP theory, are about the same, the experimental data for the pentane-quartz-vapor system are also plotted on the same graph. Both Table 2 and Fig. 8 clearly demonstrate that our experimentally obtained values of B and the disjoining pressures for the two liquids in the quartz cell are very close to that predicted from the exact DLP theory. However, we note that the value of B does vary from point to point because a real solid-liquid interface has local variations in properties.

Table 1 : Selected characteristics of pentane meniscus

	Angle of Inclination = 5.67°				Angle of Inclination = 9.92°			
	δ_0 (mn)	$K_\infty \times 10^3$ (m^{-1})	α	B (Jm)	δ_0 (nm)	$k_\infty \times 10^{-3}$ (m^{-1}	α	B (Jm)
Point A	22.0	2.512	1.12	1.43×10^{-29}	19.0	3.044	1.04	0.72×10^{-29}
Point B	20.0	3.147	1.04	0.91×10^{-29}	20.0	4.186	1.12	1.63×10^{-29}

Table 2 : Experimental and theoretically calculated values of B(∂) for pentane and heptane on quartz

n-pentane				n-heptane			
Angle ($^\circ$)	δ_0 (nm)	B_{expt} (Jm)	B_{DLP} (Jm)	Angle ($^\circ$)	δ_0 (nm)	B_{expt} (Jm)	B_{DLP} (Jm)
5.67	22.0	1.43×10^{-29}	1.14×10^{-29}	6.24	24.0	2.60×10^{-29}	1.07×10^{-29}
	20.0	0.91×10^{-29}	1.11×10^{-29}		23.0	1.57×10^{-29}	1.05×10^{-29}
9.92	19.0	0.72×10^{-29}	1.09×10^{-29}	9.92	23.0	2.41×10^{-29}	1.05×10^{-29}
	20.0	1.63×10^{-29}	1.11×10^{-29}		22.0	2.71×10^{-29}	1.04×10^{-29}

Similar results were obtained by Gee et al. (1989) from adsorption studies of n-alkanes on quartz for high disjoining pressure regimes ($\delta \leq 40\text{Å}$) and by Blake (1975), who measured the disjoining pressure as a function of film thickness for n-octane and n-decane on α-alumina. Blake's techniques demonstrated that Lifshitz theory correctly predicts the results in the low disjoining pressure regimes (δ was between 250Å and 800Å, whereas our present study is concerned with adsorbed film thicknesses of about 200Å. For completeness, we also note that recent studies by Beaglehole et al. (1991) and Beaglehole and Christenson (1992) demonstrate the limitations of the DLP theory in predicting the interactions in very thin liquid films (below 20Å). Their results suggest that structural effects are present in some adsorbed films at room temperature, provided the substrates are smooth and homogeneous.

The most important point of the present study is that the dispersion constants for a micro heat pipe system were evaluated in situ at the start of the experiments. This is a definite improvement over previous studies of micro heat pipes where little attention was given to the values of dispersion constants which are a strong function of the previous history of the substrate used in the experiments. These constants characterize the interfacial force field and are profoundly important in the basic understanding of the operation and performance of a micro heat pipe. For example, it has been shown that the contact line region in an extended evaporating meniscus, where the intermolecular force effects are important, plays a critical role in evaluating the overall heat transfer and liquid flow rates (Potash and Wayner, 1972, Wayner, 1991, Stephan and Busse, 1992, Swanson and Peterson, 1993, Schonberg et al., 1993). Hence our isothermal measurements are critical to the subsequent non-isothermal experiments.

CONCLUSIONS

1. The use of IAI in conjunction with a CVBT in a gravitational field under isothermal conditions was demonstrated.
2. Procedures to measure the dispersion constant in-situ for the vapor-liquid-solid system were developed.
3. Good agreement between theoretical and experimental values of the dispersion constant was obtained.

4. The augmented Young-Laplace equation accurately models the change in the effective pressure at the liquid-vapor interface for the systems tested.

ACKNOWLEDGEMENTS

REFERENCES

Beaglehole, D., Radlinska, E. Z., Ninham, B. W., and H. K. Christenson, 1991, "Inadequacy of Lifshitz Theory for Thin Liquid Films", *Phys. Rev. Lett.*, Vol. 66, No. 16, pp. 2084-2087.

Beaglehole, D., and H. K. Christenson, 1992, "Vapor Adsorption on Mica and Silicon : Entropy Effects, Layering and Surface Forces", *J. Phys. Chem.*, Vol 96, pp. 3395 - 3403.

Blake, T. D., 1975, "Investigation of Equilibrium Wetting Films of n-alkanes on α-alumina", *J. Chem. Soc., Faraday Trans. 1*, Vol. 71, pp. 192-208.

Brown, J. R., Chang, W. S., Halliman, K. P., and Chebaro, H. C., 1993, "Heat Transfer from Stable, Evaporating Thin Films in the Neighborhood of a Contact Line", 93-HT-4, *Proc. of Natl. Heat Trans. Conf.*, Atlanta, GA.

Cotter, T. R.,1984, "Principles and Properties of Micro Heat Pipes", *Proc. 5th Int'l Heat Pipe Conf.*, Tankuba, Japan, pp. 328-335.

DasGupta, S., Schonberg, J. A., Kim., I., Y., and Wayner, P. C. Jr., 1993a, "Use of the Augmented Young-Laplace Equation to Model Equilibrium and Evaporating Extended Menisci", *J. Colloid Interface Sci.*, Vol. 157, pp. 332-342.

DasGupta, S., Schonberg, J. A., and Wayner, P. C., Jr., 1993b, "Investigation of an Evaporating Extended Meniscus Based on the Augmented Young-Laplace Equation", *J. Heat Transfer*, Vol. 115, pp. 201-208.

DasGupta, S., Sujanani, M., and Wayner, P.C., Jr., 1991, "Microcomputer Enhanced Optical Investigation of an Evaporating Liquid Film Controlled by a Capillary Feeder", *Proc. of the 2nd World Conf. on Expt. Heat Trans., Fluid Mech. & Thermo.*, Keffer, J. F. et al. ed., Elsevier, New York, pp. 361-368.

DasGupta, S., Kim, I.Y., and Wayner, P.C., Jr., 1994, "Use of the Kelvin-Claypeyron Equation to Model an Evaporating Microfilm", accepted for publication in the *J. Heat Transfer.*

Derjaguin and Kussakov, 1939, *Acta Physicochim URSS*, Vol. 10 pp 25.

Derjaguin, B. V., Nerpin, S. V., and Churaev, N. V., 1965, "Effect of Film Transfer upon Evaporation of Liquids from Capillaries", *Bulletin Rilem*, NO. 29, pp 93-98.

Derjaguin, B.V., and Churaev, N.V., 1976, "The Definition of Disjoining Pressure and its Importance in the Equilibrium and Flow of Thin films," *Colloid J. USSR*, Vol. 38, pp. 438-448.

Dzyaloshinskii, I. E., Lifshitz, E. M., and Pitaevskii, L. P., 1961. "The General Theory of van der Waals Forces', *Ad. Phys.*, Vol. 10, 165-209.

Gee, M.L., Healy, T.W., and White, L.R., 1989, "Ellipsometric Studies of Alkane Adsorption on Quartz," *J. Colloid Interface Sci.*, Vol. 131, No. 1, pp. 18-23.

Hamaker, H. C., 1937, "The London-van der Waals Attraction Between Spherical Particles", *Physica*, Vol. 4, pp. 1058-1072.

Holm, F. W., and Goplen, S. P., 1979, "Heat Transfer in the Meniscus Thin-Film Transition Region", *J. Heat Transfer*, Vol. 101 pp. 543-547.

Hough, D. B, and White, L. R., 1980, "The Calculation of Hamaker Constants from Lifshitz Theory with Applications to Wetting Phenomena", *Adv. Coll. Interface Sci.*, Vol. 14, pp. 3-41.

Kamotani, Y., 1978, "Evaporator Film Coefficients of Grooved Heat Pipes", *Proc. 3rd Int. Heat Pipe Conf.*, Palo Alto, CA.

Khrustalev, D., and Faghri, A., 1993, "Thermal Analysis of a Micro Heat Pipe", *Proc. of Natl. Heat Trans. Conf.*, Atlanta, GA.

Lifshitz, E. M., 1955, "Theory of Molecular Attractions Between Solid Bodies", *J. Exp. Theor. Phys. USSR*, Vol. 29, pp. 94-110.

Moosman, S. and Homsy, S.M., 1980, "Evaporating Menisci of Wetting Fluids", *J. of Coll. & Interface Sci.*, Vol. 73, pp. 212-223.

Potash, M., Jr. and Wayner, P.C., Jr., 1972, "Evaporation from a Two-Dimensional Extended Meniscus," *Int. J. Heat Mass Transfer*, Vol. 15, pp. 1851-1863.

Renk, F., Wayner, P.C., Jr., and Homsy, G.M., 1978, "On the Transition between a Wetting Film and a Capillary Meniscus," *J. of Colloid and Interface Sci.*, Vol. 67, pp. 408-414.

Schonberg, J. A., DasGupta, S., and Wayner, P. C., 1993, "An Augmented Young-Laplace Model of an Evaporating Meniscus in a Micro-Channel with High Heat Flux", *Aerospace Heat Exchanger Technology 1993*, R. K. Shah and A. Hashemi (Eds.), Elsevier, pp. 239-254.

Stephan, P.C. and Busse, C.A., 1992, "Analysis of the Heat Transfer Coefficient of Grooved Heat Pipe Evaporator Walls", *Int. J. Heat Mass Transfer*, Vol. 35, pp. 383-391.

Swanson and Herdt, 1992, "Model of the Evaporating Meniscus in a Capillary Tube", *J. Heat Transfer*, Vol. 114, pp. 434-441.

Swanson, L. W., and Peterson, G. P., 1993, "The Interfacial Thermodynamics of the Capillary Structures in Micro Heat Pipes", *Proc. of Natl. Heat Transfer Conf.*, Aug. 8-11, Atlanta, GA.

Teletzke, G. F., Scriven, L. E., and Davis, H. T., 1987, "How Liquids Spread on Solids", *Chem. Eng. Comm.*, Vol. 55, pp. 41-81.

Truong, J.G. and Wayner, Jr., P.C., 1987, "Effect of Capillary and Van der Waals Dispersion Forces on the Equilibrium Profile of a wetting Liquid : Theory and Experiment", *J. Chem. Phys.*, Vol. 87, pp. 4180-4188.

Wayner, P.C., Jr., Kao, Y.K., and LaCroix, L.V., 1976, "The Interline Heat Transfer Coefficient of an Evaporating Wetting Film" *Int. J. Heat Mass Transfer*, Vol. 19, pp. 487-492.

Wayner, Jr., P.C., 1991, "The Effect of Interfacial Mass Transport on Flow in Thin Liquid Films", *Colloids and Surfaces*, Vol. 52, pp. 71-84.

Wu, D. and Peterson, G. P., 1991, "Investigation of the Transient Characteristics of a Micro Heat Pipe," *J. Thermophysics*, Vol. 5, pp. 129-134.